



**QUEEN'S  
UNIVERSITY  
BELFAST**

## **Evolution of bridge frequencies and modes of vibration during truck passage**

Cantero, D., Hester, D., & Brownjohn, J. (2017). Evolution of bridge frequencies and modes of vibration during truck passage. *Engineering Structures*, 152, 452-464. <https://doi.org/10.1016/j.engstruct.2017.09.039>

**Published in:**  
Engineering Structures

**Document Version:**  
Peer reviewed version

**Queen's University Belfast - Research Portal:**  
[Link to publication record in Queen's University Belfast Research Portal](#)

### **Publisher rights**

Copyright 2017 Elsevier.

This manuscript is distributed under a Creative Commons Attribution-NonCommercial-NoDerivs License

(<https://creativecommons.org/licenses/by-nc-nd/4.0/>), which permits distribution and reproduction for non-commercial purposes, provided the author and source are cited.

### **General rights**

Copyright for the publications made accessible via the Queen's University Belfast Research Portal is retained by the author(s) and / or other copyright owners and it is a condition of accessing these publications that users recognise and abide by the legal requirements associated with these rights.

### **Take down policy**

The Research Portal is Queen's institutional repository that provides access to Queen's research output. Every effort has been made to ensure that content in the Research Portal does not infringe any person's rights, or applicable UK laws. If you discover content in the Research Portal that you believe breaches copyright or violates any law, please contact [openaccess@qub.ac.uk](mailto:openaccess@qub.ac.uk).

1  
2  
3  
4  
5  
6  
7  
8  
9  
10  
11  
12  
13  
14  
15  
16  
17  
18  
19  
20  
21  
22  
23  
24  
25  
26  
27  
28  
29  
30  
31  
32  
33

**Title**

Evolution of bridge frequencies and modes of vibration during truck passage

**Authors**

Daniel Cantero (1)

David Hester (2)

James Brownjohn (3)

**Affiliations**

1) Department of Structural Engineering, Norwegian University of Science & Technology  
NTNU, Trondheim, Norway

2) School of Natural and Built Environment, Queen’s University Belfast, Northern Ireland.

3) Vibration Engineering Section, University of Exeter, Kay Building North Park Road, EX4  
4QF

**Abstract**

This paper reports an experimental campaign that aims at measuring the evolution of bridge modal properties during the passage of a vehicle. It investigates not only frequency shifts due to various vehicle positions, but also changes in the shape of the modes of vibration. Two different bridges were instrumented and loaded by traversing trucks or trucks momentarily stationed on the bridge. The measurements were analysed by means of an output-only technique and a novel use of the continuous wavelet transform, which is presented here for the first time. The analysis reveals the presence of additional frequencies, significant shifts in frequencies and changes in the modes of vibration. These phenomena are theoretically investigated with the support of a simplified numerical model. This paper offers an interpretation of vehicle-bridge interaction of two particular case studies. The results clearly show that the modal properties of the vehicle and bridge do change with varying vehicle position.

**Keywords**

vehicle-bridge interaction, modal analysis, nonstationary, wavelet

## 34 1. Introduction

35

36 It is a well-known fact that the modal properties of two separate mechanical systems change  
37 when both systems interact. The coupled arrangement might have significantly different  
38 natural frequencies and modes of vibrations, compared to the uncoupled systems [1]. This is  
39 also acknowledged in bridge engineering to some extent, when investigating vehicles  
40 crossing the structure, i.e. it is understood that natural frequencies of a bridge change when  
41 heavy (massive) traffic traverses it.

42

43 As pointed out by Frýba [2] the fundamental frequency of a loaded beam depends not only on  
44 the magnitude of the mass on the deck but also on the position of the mass. A key factor in  
45 the scale of frequency variation that occurs for different mass positions is the ratio between  
46 the vehicle and bridge masses, with higher mass ratios producing larger shifts in the bridge  
47 frequency. Despite the general acceptance that such frequency shifts will occur, this is a  
48 problem not well studied in bridge engineering literature [3]. However, there have been some  
49 recent studies, for example [4] describes changes in the fundamental frequency of a railway  
50 bridge during passage of a train and provides an approximate formula to calculate changing  
51 bridge frequency. Yang et al. [3] study the variation of both vehicle and bridge frequencies  
52 and present a closed-form expression for a simply supported bridge considering only the first  
53 mode of vibration. Cantero & OBrien [5] investigate numerically the effect of different mass  
54 ratios and frequency ratios on the changes in system frequencies, where frequency ratio (FR)  
55 = vehicle frequency / bridge frequency and mass ratio (MR) = vehicle mass / bridge mass.  
56 The numerical analyses of coupled vehicle-bridge models in [5, 6] show that for certain mass  
57 and frequency ratios it is possible to achieve positive frequency shifts in the fundamental  
58 frequency of the bridge. There exist only a limited number of studies that investigate this  
59 problem either experimentally, or in real operational bridges. For instance, in [7] the authors  
60 use a variety of output-only techniques with the response of a scaled model and are able to  
61 obtain clear frequency evolution diagrams for the case of large mass ratios. Also [6] performs  
62 a controlled laboratory experiment obtaining frequency shifts that validate an approximate  
63 closed-form solution of the frequency shift. The study in [8] investigates how a parked  
64 vehicle on an operational bridge affects its fundamental frequency, reporting frequency  
65 reductions of 5.4%. More recently, [9] explores the non-stationary nature of a 5-span bridge  
66 traversed by a truck, using alternative time-frequency tools, with limited success. Frequency  
67 is not the only modal property changing with load and its position; for instance [10] used

68 numerical simulation to show that damping of a pedestrian bridge also changes according to  
69 number and location of pedestrians. That said, the majority of the limited papers available on  
70 the topic focus only on tracking frequency changes and do not evaluate the effect of load on  
71 the associated mode shapes.

72

73 Although a small number of authors have used numerical models to study the problem of  
74 frequency variation with load position, to date, no experimental investigation on full scale  
75 bridges has been presented. Such a study is the main contribution of this paper. Two separate  
76 experiments were carried out, each using a different test truck on different instrumented  
77 bridges. Bridge A is a three-span continuous structure monitored while a truck traverses it at  
78 a constant speed. The measurements from Bridge A provide only weak evidence of the  
79 evolution of the modal properties and hence it constitutes only a first attempt. A second  
80 experiment is reported on Bridge B, which is a single span bridge. For the experiment on  
81 Bridge B, a truck stops at certain locations on the bridge. The free vibration measurements of  
82 the bridge accelerations, right after the vehicle stops, allows for the precise extraction of the  
83 modal parameters of the coupled system. This is repeated for various vehicle stopping  
84 positions to obtain the variation of the modal properties with respect to vehicle position. It is  
85 important to note that the variation in modal properties reported here are specific to the two  
86 case studies investigated; since these variations strongly depend on the particular vehicle and  
87 bridge.

88

89 Over the course of the investigation, it is shown that a vehicle being present on the bridge  
90 results in a coupled system, such that modal analysis results cannot be interpreted as two  
91 separate systems (bridge and truck). The vehicle-bridge interaction is a non-stationary  
92 problem where the modal parameters change with vehicle location. In general, the ideas and  
93 results presented here are of interest to engineers and researchers involved in any vehicle-  
94 bridge interaction study. However, the findings reported here have particular consequences  
95 for the current research thread on extracting bridge modal properties from passing  
96 instrumented vehicles, e.g. [11-13]. In general, these publications acknowledge that there is  
97 vehicle-bridge coupling, but fail to consider the changes in modal properties with vehicle  
98 position. In these papers modal analysis techniques are often applied to the full length of the  
99 signal obtained during vehicle passage. However, attempting to analyse what is in effect a  
100 non-stationary signal with conventional modal analysis techniques developed for stationary  
101 signals will necessarily result in unreliable modal properties.

102

103 As well as demonstrating that the bridge acceleration signal recorded during the passage of a  
104 truck is non-stationary, this paper provides advice and insight on a number of related issues.  
105 First, a modified and novel approach for performing the Continuous Wavelet Transform  
106 (CWT) is presented, and is shown to be an effective signal processing technique to visualise  
107 variations in system frequencies. Next, the source of the additional frequency peak in the  
108 spectra of the forced (i.e. loaded) bridge acceleration signal is investigated. This is carried out  
109 using a relatively simple but insightful numerical model, and experimental data from Bridges  
110 A and B. Moreover, this paper shows for the first time that not only do the natural  
111 frequencies evolve during traffic passage, but that the shapes of the associated modes of  
112 vibration also evolve. For every vehicle location, the vehicle-bridge system features distinctly  
113 different modes. This is supported by a theoretical analysis of the problem, and carefully  
114 extracted experimental results. However, it should be noted that this paper only reports  
115 findings on the first longitudinal mode of the bridge, no torsional or higher modes are  
116 investigated.

117

118 The remainder of this paper has four primary sections. Section 2 provides a theoretical  
119 background on the numerical model, modal analysis, and signal processing techniques used  
120 in this study. Section 3 describes an experimental test where a truck was driven across a 3-  
121 span bridge. Additional frequencies were observed in the spectra of the recorded bridge  
122 response. A numerical model is used to postulate the origin of the additional frequency peak.  
123 However, to experimentally confirm the validity of the model predictions it was necessary to  
124 redo the experiment using a revised procedure where the truck would stop at a series of  
125 discrete locations on a bridge. The outcome of the revised experiment is reported in Section  
126 4.

127

## 128 **2. Methods**

129

130 This section provides the reader a brief overview of the tools used throughout this study.  
131 Section 2.1 describes the numerical model that helps explain non-intuitive changes in modal  
132 properties observed in the experiments. Section 2.2 provides references on the modal analysis  
133 procedures employed to analyse the measured acceleration signals. Finally, Section 2.3  
134 describes a modified form of wavelet analysis that is used to visualise variations in the  
135 system frequencies for the non-stationary acceleration signals recorded on site.

136  
137  
138  
139  
140  
141  
142  
143  
144  
145  
146  
147  
148  
149  
150  
151  
152  
153  
154  
155  
156  
157

## 2.1 Numerical model

The coupled vehicle-bridge model was programmed in Matlab [14] and a pictorial representation of the numerical model is shown in Fig. 1. The truck is simulated as a sprung mass  $m$  supported on a spring  $k$ , where the spring represents the suspension of the vehicle. The bridge is simulated using a finite element beam model where each beam element has 4 degrees of freedom, namely a rotation and a vertical translation at each end of the element. Elemental matrices for this kind of element can be found in the literature, e.g. [15]. The beam is defined by its span  $L$ , section area  $A$ , modulus of elasticity  $E$ , second moment of area  $I$  and mass per unit length  $\rho$ . The location of the vehicle is defined by the distance from the left support ( $x$ ) and in the simulations the vehicle can be positioned anywhere on the beam ( $0 \leq x \leq L$ ). The coupling between both systems, i.e. bridge and vehicle, can be written in terms of the beam element shape functions and the relative position of the vehicle within that element [16]. However, defining a sufficiently dense mesh that has a node exactly at the location of the vehicle reduces the complexity of the procedure. In that case the matrices of both systems are assembled diagonally, and the coupling terms are off-diagonal negative stiffness values that link together the appropriate degrees of freedom. As two different bridges will be modelled, (each with different boundary conditions), for now the boundary conditions of the model are indicated with question marks in Fig. 1. Models of this type have previously been presented in the literature [17].

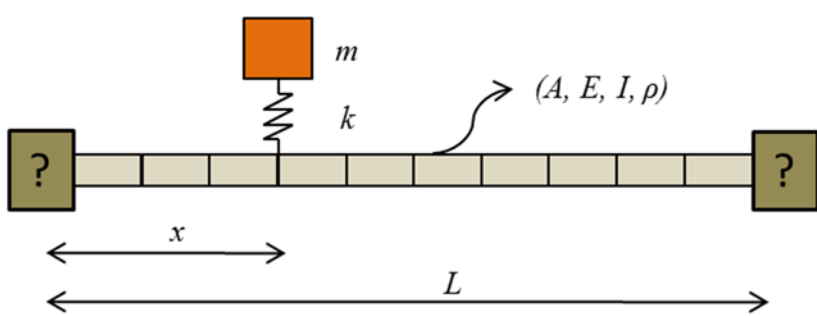


Fig. 1: Coupled Vehicle-Bridge finite element model

158  
159  
160  
161  
162  
163  
164

Fundamentally, the purpose of this model is to allow the vehicle to be moved incrementally across the bridge and to track how the bridge frequency changes with the position of the vehicle. For a given vehicle position, the bridge frequencies and associated modes of vibration can be determined using an eigenvalue analysis. Simulating a multi-axle truck as a

165 single degree of freedom sprung mass is a simplification, and for some applications it would  
 166 be an over simplification. However, it is shown later that for the purpose of this study, where  
 167 the primary interest is in explaining the evolution of frequency with respect to truck position,  
 168 the model is effective. Initially values for area ( $A$ ), second moment of area ( $I$ ) and mass per  
 169 unit length ( $\rho$ ) were determined from the available bridge drawings. For the Young's  
 170 Modulus ( $E$ ), standard values for steel and concrete of  $2 \times 10^{11}$  N/m<sup>2</sup> and  $2 \times 10^{10}$  N/m<sup>2</sup>  
 171 respectively were used. After getting an initial estimate of bridge frequencies from the model,  
 172 the bridge properties (in the model) are revised so that the fundamental bridge frequency of  
 173 the model matches the free vibration frequency observed on site, this is further described in  
 174 Sections 3 and 4. For the vehicle, the spring stiffness ( $k$ ) is adjusted so that the vehicle  
 175 frequency in the model matches the vehicle frequency inferred from the acceleration  
 176 measurements recorded experimentally when the truck was traversing the real bridge. Table 1  
 177 gives a summary of relevant information about the vehicle and bridge properties used in this  
 178 paper. It can be seen in Table 1 that the vehicle properties postulated for the test vehicles  
 179 give body bounce frequencies that are in accordance with typical values for heavy vehicles  
 180 (1 Hz to 4 Hz) as shown in [18].

181

182 Table 1: Vehicle and bridge properties

		Test on Bridge A	Test on Bridge B
Bridge	Type	3-span continuous	1-span
	Spans (m)	18+31+18	36
	$f_b$ (Hz)	3.50	3.13
Vehicle	Mass (kg)	26 000	32 000
	$f_v$ (Hz)	2.80	2.60
	Number of axles	3	4
	Axle distances (m)	1.4+4.1	2.0+3.5+1.4
	Velocity (m/s)	3.63	-

183

## 184 2.2 Bridge modal analysis

185

186 The Introduction provided an overview of literature dealing with variation in bridge  
 187 frequency with respect to variation in mass distribution. It was also highlighted that previous  
 188 studies have not looked at how the mode shapes associated with these frequencies change  
 189 with respect to variation in mass distribution. To address this limitation this study attempts to  
 190 experimentally capture the mode shape associated with a particular truck position. This is  
 191 achieved using output-only modal analysis methods, i.e. no information on the excitation is

192 measured. Due to the size/mass of road bridges, output-only methods are often the only  
193 logistically feasible approach to extract modal parameters, because using shakers or impact  
194 hammers to excite the structure is often not practical. Specific details on the theory/  
195 mathematics underlying output-only modal analysis are not provided here as the topic has  
196 been extensively covered in other publications such as [19]. The particular method used in  
197 this paper is Frequency Domain Decomposition (FDD) and details on this method are given  
198 in [20].

199

### 200 **2.3 Wavelets**

201

202 To be able to accurately visualise the variation in frequency with respect to time, some time-  
203 frequency representation of the recorded signals is necessary. There are a number of time-  
204 frequency analysis methods available, e.g. Short Time Fourier Transform, Hilbert-Huang  
205 transform and Wavelet transform. Within each of these methods, different options in their  
206 implementation can significantly change the time-frequency plots that are output. All time-  
207 frequency analysis methods involve a trade-off in resolution, i.e. high resolution in the  
208 frequency domain typically means poor resolution in the time domain, and vice versa.  
209 Ultimately, it is up to the analyst to identify which method best achieves their objective. In  
210 this paper, the objective of the time-frequency analysis is to visualise how the bridge  
211 frequency changes as a truck traverses the bridge.

212 In essence, the CWT compares the wavelet bases (a wave-form of finite length) to the  
213 analysed signal and gives a wavelet coefficient, so that the better the match, the larger the  
214 coefficient. This wavelet is then shifted in time to cover the whole length of the signal,  
215 resulting in a vector of wavelet coefficients. The wavelet is then scaled (i.e. stretched) and the  
216 process is repeated. For each scale used in the analysis a vector of wavelet coefficients  
217 results. Scale can be regarded as inversely proportional to frequency and thus can be  
218 transformed approximately to frequency, or more specifically pseudo-frequency. The result  
219 of CWT analysis is a plot of wavelet coefficients in the time-frequency plane that are  
220 proportional to the energy of the signal. For additional information on wavelets and to find a  
221 full mathematical description further details are provided by other authors [21,22].

222

223 When using the CWT, several wavelet basis functions are available, e.g. Morlet, Gaussian,  
224 Mexican hat. The results from the CWT are significantly affected by the wavelet basis used  
225 in the analysis so it is paramount to choose an appropriate basis. Knowing which wavelet



226 basis will give the best results for a given application is not always obvious, and often there is  
227 a degree of trial and error involved. However, [23] showed that the Modified Littlewood-  
228 Paley (MLP) wavelet basis was effective when analysing the acceleration signals of bridges  
229 subject to vehicle loading, and therefore this is the wavelet basis used in this study.

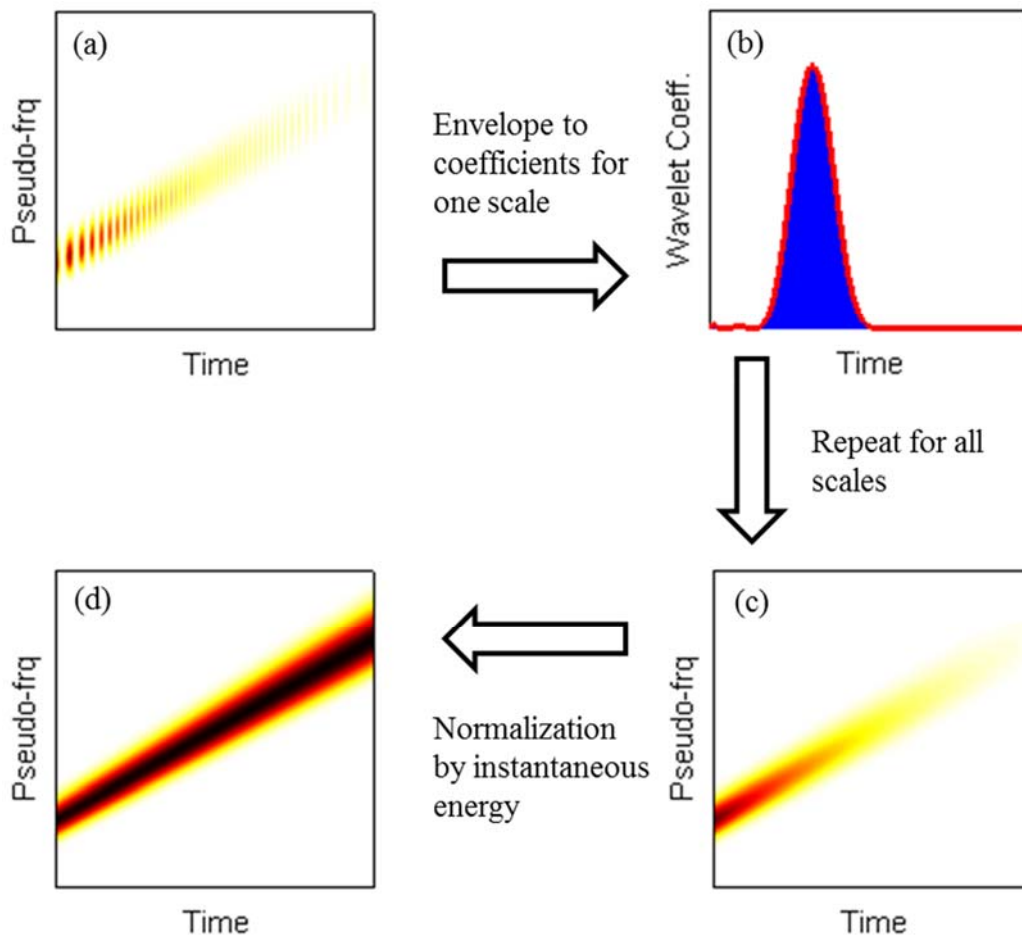
230

231 In addition, this paper proposes a non-conventional normalisation step that proves very  
232 effective when analysing bridge signals that contain a mixture of free and forced vibration.  
233 Using a conventional CWT to analyse a bridge signal that has both free and forced vibration  
234 can be difficult. The forced vibration part of the signal has the largest amplitude, and as a  
235 result this will dominate the resulting CWT plot. This makes it very difficult to track the  
236 frequency evolution between the free and forced parts of the signal because the frequency  
237 from the free vibration part will be practically invisible. The novel procedure adopted here  
238 gets around this problem by normalising the wavelet coefficients at each time instant and is  
239 presented schematically in Fig. 2.

240

241 A signal with linearly increasing frequency and linearly decreasing amplitude is analysed  
242 with a conventional CWT and the result is shown in Fig. 2(a). The plot represents a 3D  
243 wavelet surface as a 2D ‘contour’ plot where the magnitude of the wavelet coefficients are  
244 conveyed using colour, with darker colours implying large values of wavelet coefficient. The  
245 non-stationarity property and decreasing amplitude of this numerically generated signal can  
246 clearly be appreciated in the plot. Unfortunately, from the point of view of frequency  
247 tracking, the large amplitudes in the early part of the signal are resulting in high wavelet  
248 coefficients that are in a sense dominating the plot and making it difficult to see the frequency  
249 content in the latter part of the signal. However, if one is prepared to sacrifice information  
250 relating to amplitude, which for the purpose of this paper we are not concerned with, then this  
251 representation can be improved. The first step is to fit an envelope to the wavelet coefficients  
252 for a given scale and to accept this curve as the representative result from the CWT. An  
253 example of this curve fitting is shown in Fig. 2(b). The blue plot in Fig. 2(b) shows the  
254 wavelet coefficients at a particular scale, the red curve has been fitted to the blue plot. If a  
255 similar curve is fitted at every scale, and then if all the ‘fitted’ curves are plotted in 2D, the  
256 plot shown in Fig. 2(c) results. The second step is to normalise each wavelet coefficient at a  
257 given time instant by the total energy content for that time instant. The result of applying this  
258 normalisation is shown in Fig. 2(d). The consequence of this normalization is that it gives the  
259 same importance to the frequency of small amplitude vibrations as it does to the frequency of

260 large amplitude vibrations. The usefulness of this normalization will become clear when  
 261 studying the measured accelerations in Sections 3 and 4 below. Obviously, the substitution by  
 262 the envelope curve and then later application of normalization comes with a cost. The final  
 263 map of wavelet coefficients cannot be used for signal reconstruction. However, for  
 264 visualization purposes these two operations greatly improve the final result from the CWT.  
 265



266

267

Fig. 2: Enhancement of energy map from CWT analysis

268

### 269 3. Experimental study of Bridge A and moving truck

270

271 This section describes the first experimental investigation carried out on a 3-span road bridge.  
 272 A truck is driven over the bridge and the bridge acceleration is recorded at a number of  
 273 locations. This acceleration data is subsequently analysed to examine how the modal  
 274 parameters of the bridge change as the truck crosses the bridge. Section 3.1 describes the  
 275 bridge and experiment setup used. Section 3.2 presents the results of modal analysis carried  
 276 out on free and forced vibration data. Finally, Section 3.3 puts forward a theoretical model to

277 explain the behaviour observed in Section 3.2. Note that this experiment on Bridge A is only  
278 the first attempt to study the evolution of modal properties during vehicle passage and a  
279 plausible explanation is provided based only on weak evidence. A second experiment that  
280 provides stronger evidences is performed on a different bridge and is reported in Section 4.

281

### 282 **3.1 Bridge and instrumentation description**

283

284 The bridge used in the experiment is shown in Fig. 3(a). It is a 3-span bridge carrying a minor  
285 road (4 m wide) over a dual carriageway. The deck consists of 2 steel girders supporting a  
286 concrete deck. The centre span is 31 m and each of the side spans are 18 m. There were two  
287 primary reasons for selecting this bridge. Firstly, the bridge deck is relatively light, narrow  
288 carriageway and primary members are steel. This is advantageous because a high (vehicle-  
289 bridge) mass ratio should lead to larger changes in modal properties. The second reason for  
290 selecting this bridge is that the traffic volumes on the bridge are very light, which made it  
291 logistically feasible to carry out the test. The vehicle used in the test is a 3-axle truck with a  
292 total mass of 26 tonnes, shown in Fig. 3(b). The truck crossed the bridge twice (once in each  
293 direction) at a crawling speed of approximately 13 km/h (3.63 m/s). Such a low speed  
294 effectively reduces the dynamic effects associated with (i) road profile unevenness, (ii)  
295 loading frequencies due to the vehicle's axle spacing and (iii) shifting of bridge frequencies  
296 [24]. Despite the low speed the truck still provides sufficient excitation to the system.

297



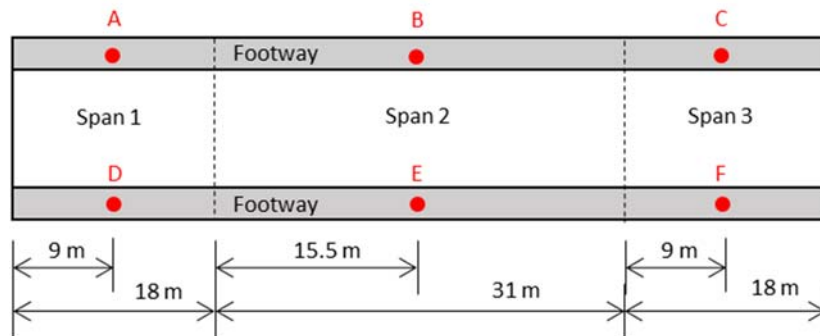
298 Fig. 3: (a) Bridge A elevation (3-span bridge); (b) Truck used in experiment

299

300 Fig. 4 shows a plan view of the bridge deck. The position of the piers is indicated using  
301 dashed lines and for convenience the spans are labelled as spans 1-3. The bridge has a 4 m  
302 wide carriageway with 0.5 m wide footways on either side. Due to the impossibility of road  
303 closure, the instrumentation had to be installed on the footway and it was installed as close as  
304 possible to centre of the main beams. The location of the six accelerometers (A-F) used in the

305 test are indicated in Fig. 4. One accelerometer was placed at mid-span of each of the three  
 306 spans on both sides of the bridge. The accelerometers used were tri-axial Micro-Electro  
 307 Mechanical System (MEMS) accelerometers scanning at 128 Hz.

308



309

310

Fig. 4: Plan view and accelerometer layout on Bridge A.

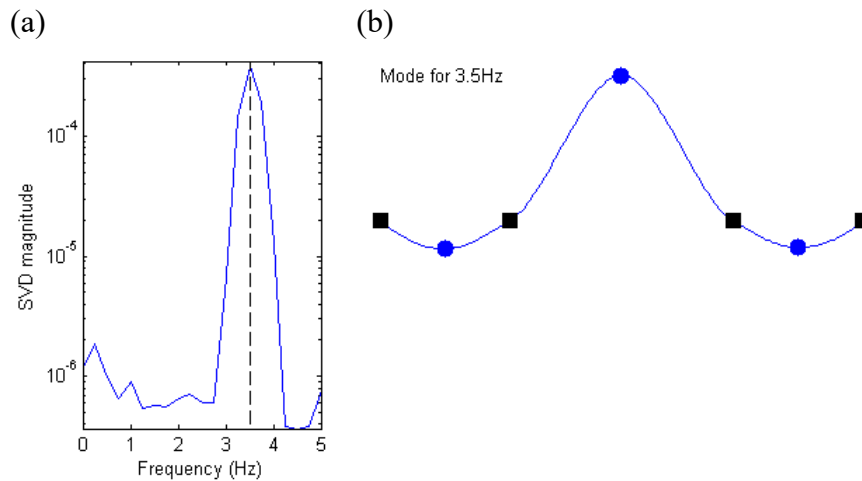
311

### 312 3.2 Modal analysis of free and forced vibration data

313

314 The first step in analysing the data is to perform modal analysis on the free vibration data, i.e.  
 315 no truck on the bridge. The FDD modal analysis approach described in Section 2.2 is used to  
 316 analyse the free vibration data. Singular Value Decomposition (SVD) of the Power Spectral  
 317 Density matrix is plotted in Fig. 5(a) where a clear peak is visible at 3.5 Hz indicating the  
 318 likely presence of a mode. Note that the poor frequency resolution is due to the short duration  
 319 of analysed signal. The associated mode of vibration is extracted and presented in Fig. 5(b).  
 320 The square data markers represent the bridge supports, i.e. the modal amplitude at these  
 321 locations is assumed zero. The circular data markers (from left to right) indicate the modal  
 322 amplitudes at sensor locations A, B and C, see Fig. 4. If the modal ordinates for sensor  
 323 locations D, E and F are plotted the same mode shape is apparent. Thus it is clear that the  
 324 mode at 3.5 Hz is the first bending mode. This result is consistently obtained for various  
 325 different free vibration measurements.

326



327 Fig. 5: Modal analysis of signals during free vibration of Bridge A; (a) Singular Value  
 328 Decomposition magnitude; (b) Extracted fundamental mode

329  
 330 Once the free vibration data was analysed the next step was to analyse the forced vibration  
 331 response, i.e. the acceleration recorded while the truck was on the bridge. The results of  
 332 analysing the forced vibration data is presented in Fig. 6. The analysis procedures used are  
 333 the same as those used to generate the plots in Fig. 5. However, there are in this case, some  
 334 noticeable differences in the results. The SVD analysis in Fig. 6(a) identifies the presence of  
 335 two distinct peaks at 2.63 Hz and 3.63 Hz respectively, but the fundamental bridge mode at  
 336 3.5 Hz identified in Fig. 5 is no longer evident. The mode shapes associated with the two  
 337 frequency peaks are shown in Fig. 6(b).

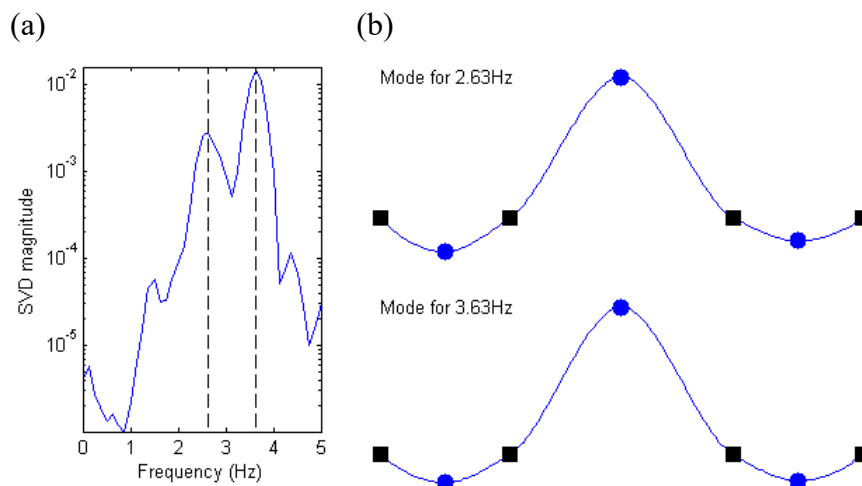
338  
 339 Starting with the mode shape for the 3.63 Hz mode, it is noticeable that it is very similar in  
 340 shape to the mode shown in Fig. 5(b), so it is reasonable to assume that this is the same mode.  
 341 However, the presence of the truck has changed the frequency of the mode slightly. It is  
 342 interesting to note that the fundamental frequency of the bridge has increased. Intuitively one  
 343 would expect a slight reduction in the frequency because the truck is adding mass to the deck.  
 344 Moving on to the mode identified at 2.63 Hz, its origins are less clear. One possibility is that  
 345 perhaps the loading frequency produced an excitation in the region of 2.63 Hz. For this truck  
 346 three possible axle spacings need to be considered, namely 1.4 m, 4.1 m and 5.5 m, which are  
 347 the distances from axle-1 to axle-2, axle-2 to axle-3, and axle-1 to axle-3 respectively. For a  
 348 traversing speed 3.63 m/s the possible loading frequencies are 0.38 Hz, 1.13 Hz and 1.52 Hz.  
 349 Another possibility is that the shift in bridge frequency is due to the driving velocity of the  
 350 vehicle, as discussed in Yang et al. [24]. This shift in frequency is directly proportional to the  
 351 vehicle speed and inversely proportional to double the bridge span. Due to the low speed of

352 the traversing vehicle, only shifts of  $\pm 0.03$  Hz in the bridge fundamental frequency can be  
353 expected. Therefore, neither the vehicle loading frequency nor the frequency shift due to  
354 driving velocity explain the frequency peak at 2.63 Hz.

355

356 Obviously, the origins of the 2.63 Hz frequency is likely to be related to the vehicle's  
357 presence, and it is reasonable to consider that the 2.63 Hz may be the vehicle frequency  
358 however, it is difficult to be definitive just on the evidence of Fig. 6. Interestingly the mode  
359 shape associated with the 2.63 Hz peak is practically a duplicate of the fundamental bridge  
360 mode identified in Fig. 5(b). Therefore, to get a better theoretical understanding of why the  
361 presence of a truck is; (i) causing a slight increase in the frequency of the fundamental mode  
362 and (ii) resulting in the appearance of a new mode, the vehicle-bridge model described in  
363 Section 2.1 is used in the next section to calculate the system frequencies for a series of  
364 different vehicle positions.

365



366 Fig. 6: Modal analysis of signals during forced vibration of Bridge A; (a) Singular Value  
367 Decomposition magnitude; (b) Extracted first and second modes

368

### 369 3.3 Theoretical model of observed behaviour

370

371 In an effort to better understand the frequencies observed in Fig. 6 the vehicle-bridge model  
372 described in Section 2.1 is used here to position the vehicle model at a series of discrete  
373 points along the length of the beam and to examine how the frequencies of the system  
374 (vehicle and bridge) are affected. The bridge is modelled as a 3-span continuous beam with  
375 restrained vertical displacements at the ends and intermediate locations, which represent the

376 support conditions at the abutments and over the piers. The bridge properties in the model are  
377 revised so that the fundamental frequency in the model is 3.5 Hz and the properties of the  
378 vehicle model have been adjusted to get a vehicle frequency of 2.8 Hz. The total mass of the  
379 vehicle in the model is 26000 kg. Although the exact frequency of the vehicle was not  
380 measured on site, based on the experimental observations in the previous section, and the  
381 information in the literature [18], a vehicle frequency of 2.8 Hz seems reasonable. It should  
382 be noted that the purpose of this model is not to exactly simulate the vehicle crossing event  
383 recorded experimentally. Instead, the purpose is to examine what happens to the bridge and  
384 vehicle frequencies if the sprung mass is placed at a series of discrete points along the length  
385 of the beam. This is achieved by positioning the sprung mass at a given point on the bridge  
386 and performing an eigenvalue analysis the system matrices of the coupled model system to  
387 identify the system frequencies for that vehicle position. Then the vehicle is consecutively  
388 moved to the next point on the bridge and the system frequencies for each new position are  
389 calculated. As the vehicle-bridge system is coupled, technically these frequencies should be  
390 termed the ‘first system frequency’, ‘second system frequency’, etc. However, for convention  
391 in the following discussion they are also referred to as ‘vehicle’ and ‘bridge’ frequencies.

392

393 The evolution of the system frequencies for various vehicle positions is presented in Fig. 7.  
394 The horizontal axis in Fig. 7 shows the position of the vehicle relative to the left support as a  
395 percentage of the total bridge length  $L$ . So when the vehicle is exactly over the left support its  
396 position is 0% of  $L$ , when it is half way across its position is 50% of  $L$ , and when it is exactly  
397 over the right support its position is 100% of  $L$ . The two dashed vertical lines in the figure at  
398 26% and 73% indicate the position of the two piers. The ordinates in Fig. 7 are frequency  
399 values. The two horizontal lines at 3.5 Hz and 2.8 Hz represent the vehicle and bridge  
400 frequencies in isolation, i.e. in the absence of any interaction between them.

401

402 The lower solid line in Fig. 7 shows the variation in the vehicle frequency as the vehicle is at  
403 various positions along the length of the bridge. Tracing this plot from left to right, it can be  
404 seen that when the vehicle is positioned over the left support its frequency (2.8 Hz) remains  
405 unchanged. However, when the vehicle is positioned toward the centre of span 1 ( $x \approx 13\%$ )  
406 the vehicle frequency drops below 2.8 Hz. Then, as the vehicle is positioned at the first pier  
407 ( $x \approx 26\%$ ), the vehicle frequency goes back up to 2.8 Hz. As the vehicle is incrementally  
408 moved toward the centre of span 2 the vehicle frequency shows a steady reduction in  
409 frequency to a minimum value of approximately 2.4 Hz at the mid-span of span 2 ( $x \approx 50\%$ ).

410 As the position of the vehicle continues toward pier 2 the vehicle frequency shows a gradual  
411 increase and it recovers completely to 2.8 Hz when the vehicle is over pier 2. A similar  
412 reduction in vehicle frequency is evident when the vehicle is positioned in the centre of span  
413 3. If the vehicle is thought of in isolation, i.e. if it is visualised as a mass supported on a  
414 spring, this pattern is difficult to understand. However, if, for the crossing event, the vehicle  
415 is thought of as a mass on two vertical springs, (one on top of the other) it is easier to  
416 understand. The upper spring being the vehicle suspension and the lower spring being the  
417 bridge, i.e. it is now a 2 degree of freedom system. The stiffness of the upper spring (the  
418 vehicle suspension) is constant. The stiffness of the lower spring (the bridge) is not constant  
419 since it depends on where the vehicle is positioned on the bridge. When the vehicle is over a  
420 bridge support the lower spring could be regarded as infinitely stiff so the vehicle behaves as  
421 an uncoupled single DOF system and the frequency remains 2.8 Hz. However, when the  
422 vehicle is at the mid-span of the bridge the lower spring is no longer infinitely stiff, as the  
423 system of springs supporting the mass is more flexible than it was before (when the vehicle  
424 was over a support) so the frequency of the system drops. Note that the 2 degree of freedom  
425 model/visualisation constitutes only an analogy that encapsulates the frequency evolution  
426 phenomena. Similar models have been reported in [25, 26] to study the dynamics of vehicle-  
427 bridge interaction systems.

428

429 Turning our attention to the upper solid line in Fig. 7, the result shows how the bridge  
430 frequency changes with respect to the position of the vehicle on the bridge. The most relevant  
431 thing about this plot is that for certain truck positions the bridge frequency is actually  
432 predicted to increase. This is counterintuitive because one would expect the bridge frequency  
433 to reduce slightly if a concentrated un-sprung mass was placed on the bridge deck. (This is  
434 indeed what would happen and this is demonstrated later in Fig. 12). However, it appears that  
435 when the moving mass is sprung, there are situations where the bridge frequency can actually  
436 increase slightly. It is conceivable that the sprung mass (truck body) adds a kind of inertial  
437 resistance to bridge's motion. In other words, the vehicle mass is providing some restraint to  
438 the upper end of the truck suspension (spring), which is touching the bridge deck. This can be  
439 interpreted as if the truck provides an extra spring support at the location the truck is located  
440 at. Obviously, from a static point of view, the number of bridge supports remains unchanged.  
441 For convenience in this paper we will term this apparent localised stiffening of the beam  
442 where the truck is parked an 'inertial spring support'. It can be seen in the upper solid line in  
443 Fig. 7 that when the truck is at either of the 2 short side spans the addition of this inertial

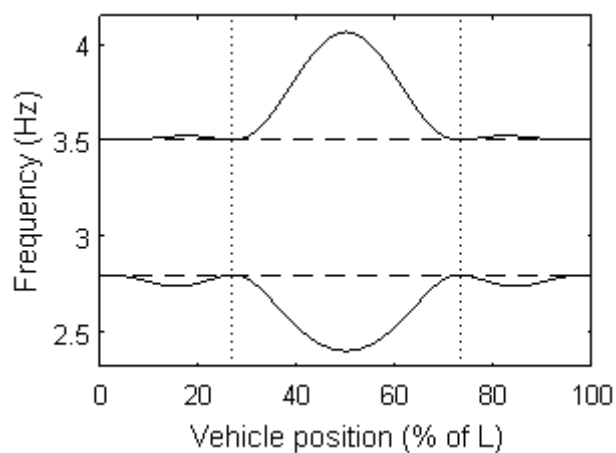


444 spring support makes very little difference to the bridge frequency, indicating that it is adding  
445 relatively little stiffness to the system. However, when the truck is on the longer central span,  
446 the addition of an ‘inertial spring support’ does result in a significant increase in frequency.

447

448 Conceptualising the body of the vehicle as described above is helpful for initial visualisation  
449 as it allows the bridge to be idealised in a conventional static structural arrangement.  
450 However, in reality the vehicle-bridge system is a dynamic system so the behaviour is more  
451 complex and insight on the behaviour is provided by [5]. Using a simple numerical model of  
452 a sprung mass on a single span beam, they investigated how the system frequencies changed  
453 as the sprung mass was positioned at different points on the beam. The results of [5] showed  
454 frequency variation patterns similar to those shown in Fig. 7. Moreover, they found that the  
455 increase and decrease in bridge and vehicle frequencies respectively was sensitive to the  
456 frequency ratio (FR), where  $FR = \text{vehicle frequency} / \text{bridge frequency}$ . For systems where  
457 the vehicle frequency was less than the bridge frequency (which is the situation here) and  
458 when FR was close to one (e.g. 0.95), their model shows that large shifts in bridge and  
459 vehicle frequencies would occur. However, when FR was not close to one (e.g. 0.5) the  
460 frequency shifts predicted by the model were significantly smaller. The difference in the  
461 magnitude of the frequency shift with respect to FR shows that it is not as simple as thinking  
462 of the truck mass as a restraint. It appears that the closer the vehicle frequency is to the bridge  
463 frequency the more pronounced this restraint is, which demonstrates the dynamic nature of  
464 the restraint. It was also shown in [5] that the frequency shifts predicted by the model were  
465 larger for higher mass ratios (MR) where  $MR = \text{vehicle mass} / \text{bridge mass}$ .

466

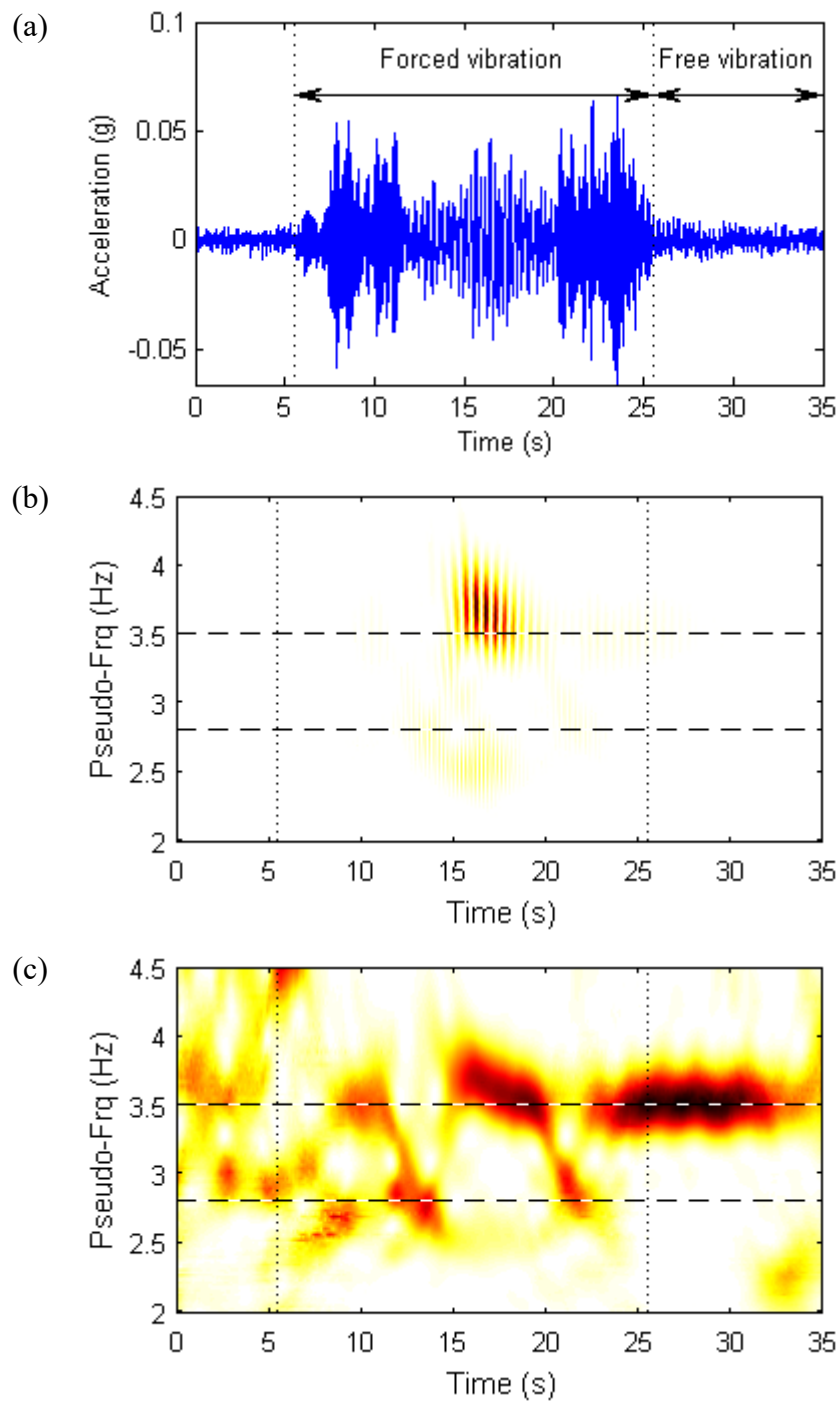


467

468 Fig. 7: Numerical frequency evolution of uncoupled system (dashed lines) and coupled  
469 system (solid lines). Vertical dotted lines indicate intermediate bridge supports.

470

471 Although the numerical model used to generate Fig. 7 is only an approximation of the real  
472 bridge, it does clearly show that the frequency content during a vehicle passage is likely to  
473 change. This variation in frequency with respect to vehicle position makes the problem non-  
474 stationary and the acceleration signals recorded during the passage of the vehicle should  
475 reflect the non-stationary nature of the process, i.e. a change in frequency should be evident.  
476 To examine if this frequency change is evident, the acceleration response from centre of span  
477 3 (sensor C in Fig. 4) is analysed using the wavelet approach described in Section 2.3.  
478 Fig. 8(a) shows the acceleration time series recorded at sensor C during a truck passing event.  
479 For this crossing event the first axle of the truck enters the bridge at 6 s and the last axle exits  
480 the bridge at 26 s. The truck entering and leaving the bridge is indicated in the figure by  
481 dotted vertical lines. Thus, the signal between these two lines corresponds to forced vibration  
482 data, whereas the acceleration after the truck leaves is the free vibration data. Fig. 8(b) shows  
483 the conventional wavelet transform of the complete time series shown in Fig. 8(a) and  
484 Fig. 8(c) shows the wavelet coefficients after calculating the envelope along scales and  
485 normalizing by instantaneous energy (see Section 2.3). In Fig. 8(b) & (c) the truck entering  
486 and leaving the bridge is again indicated using dotted vertical lines. Parts (b) and (c) of the  
487 figure also have dashed horizontal lines at 3.5 Hz and 2.8 Hz. The dashed horizontal line at  
488 3.5 Hz is the uncoupled bridge frequency and the dashed horizontal line at 2.8 Hz is believed  
489 to be the approximate uncoupled vehicle frequency. In the absence of a modal test on the  
490 vehicle, one cannot say definitively that 2.8 Hz is the vehicle frequency, but based on the  
491 numerical model and the available experimental data the authors believe this is a reasonable  
492 supposition. The conventional CWT result (Fig. 8(b)) shows only some high energy  
493 concentration within the studied frequency range when the vehicle is traversing the middle  
494 span. On the other hand, the processed wavelet coefficients (Fig. 8(c)) provide a better  
495 picture of the relative energy distribution in the time-frequency plane. The frequency  
496 evolution is not entirely clear in the CWT plot in Fig. 8(c). However, it is apparent that  
497 during free vibration the bridge is vibrating only at its fundamental frequency (3.5 Hz) as all  
498 the energy is concentrated there. On the other hand when the truck is on the bridge (forced  
499 vibration) there is also a significant amount of energy near what the authors believe to be the  
500 vehicle's first frequency (2.8 Hz). Furthermore, a trend seems to be evident in Fig. 8(c)  
501 similar to the one predicted Fig. 7. During the period 12-20 s when the vehicle is crossing the  
502 central span of the bridge the vehicle frequency seems to go down and the bridge frequency  
503 seems to go up.



505 Fig. 8: Acceleration and frequency content for truck passage on Bridge A (a) Acceleration  
 506 signal; (b) Raw CWT result; (c) Processed CWT; Vertical lines = start/end of forced  
 507 vibration; Horizontal dashed lines = uncoupled system frequencies

508

509 Although Fig. 8 partially supports the theoretical construct presented in Fig. 7, it is difficult to  
 510 draw any firm conclusions about the validity of the suggested explanations. This is because  
 511 the frequencies presented in Fig. 7 are calculated for the vehicle model being situated at a

512 series of discrete locations on the beam. Unfortunately, the experimental data in this section  
513 is for a moving truck and it could justifiably be argued that it is not correct to apply FDD to a  
514 non-stationary process to extract the modal properties. Therefore, it is not possible to reliably  
515 extract the modes of the coupled system while the vehicle is moving. This means that the  
516 frequency peaks shown in Fig. 6 are likely to be a good approximation of the real frequencies  
517 but will not be totally accurate. To overcome these issues a new experiment, where a truck is  
518 parked at a series of discrete locations on a bridge, is undertaken and this work is reported in  
519 the next section.

520

#### 521 **4. Experimental study of Bridge B and stationary truck**

522

523 As explained at the end of the previous section the experimental results from Bridge A cannot  
524 really be used to check the validity of the concept presented in Fig. 7. In the previous  
525 experiment the truck was moving, but in the numerical model the truck was parked at a series  
526 of discrete locations. To resolve this issue a second experimental campaign was undertaken  
527 where a truck was actually parked at a number of discrete locations on the bridge and the  
528 results are described herein. To make sure that the bridge behaviour observed in Section 3  
529 was not specifically related to Bridge A or the test truck shown in Fig. 3(b), in this next  
530 experiment a different bridge and truck are used. It is important to note that when a vehicle is  
531 parked on the bridge the system is coupled but stationary, i.e. the modal parameters will  
532 remain constant. Therefore, using output-only modal analysis techniques such as FDD to  
533 extract the modal properties is appropriate.

534

#### 535 **4.1 Bridge and instrumentation description**

536

537 A photo of the bridge used in this experiment is shown in Fig. 9(a) and a plan view in  
538 Fig. 10(a). The bridge is a half through steel girder bridge, it spans 36 m and the deck is  
539 simply supported. The 7.6 m wide, and 200 mm deep concrete deck is supported on a series  
540 of 450 mm deep steel beams, which span transversely between the main girders which are  
541 approximately 2 m deep. As explained in Section 3.1, for experiments of this type, a high  
542 vehicle-bridge mass ratio is desirable, so a light bridge deck is advantageous. The reason for  
543 choosing this bridge is that the deck is light compared to other bridges of the same span, i.e.  
544 the primary members are steel and the deck is relatively narrow. Again with the objective of  
545 having a high (vehicle-bridge) mass ratio, the truck selected for this test had a total weight of

546 32 tonnes, which is heavier than the 26 tonnes truck used in the previous test. The test truck  
547 used has four axles and is shown in Fig. 9(b). While the bridge was chosen for its technical  
548 advantages described above, logistically the disadvantage of the bridge was that it was in an  
549 urban area and frequently trafficked, which made finding a quiet time to carry out the test  
550 challenging.

551

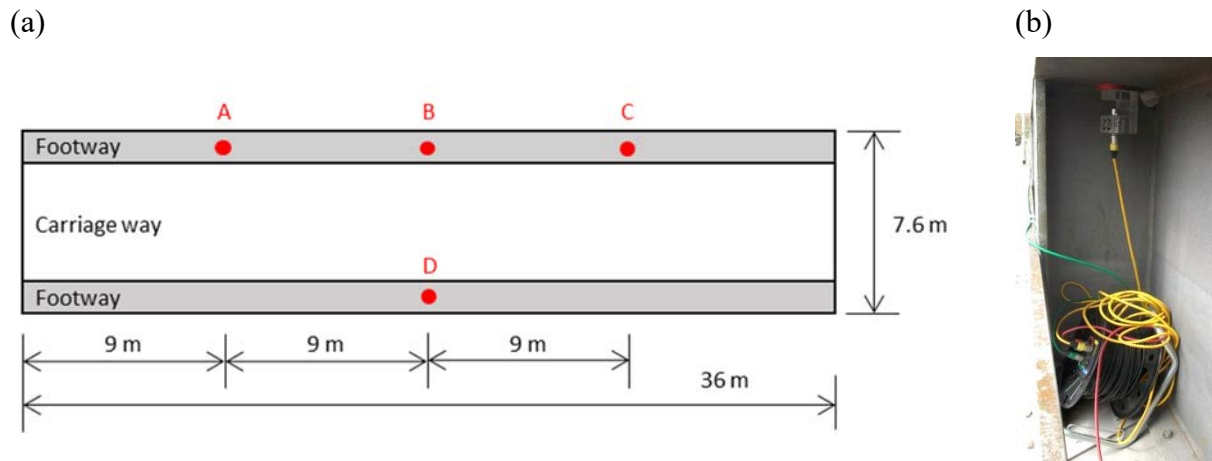


552 Fig. 9: (a) Bridge B elevation; (b) Test truck

553

554 The instrumentation used in this experiment consisted of four accelerometers attached to the  
555 main girders. The position of the four accelerometers (A-D) is shown in Fig. 10(a). The  
556 accelerometers used in this test were Honeywell QA750 force balance accelerometers and the  
557 scanning frequency used was 128 Hz. Fig. 10(b) shows accelerometer B attached to the  
558 underside of the top flange of the main girder via a magnet. The vehicle was parked for short  
559 durations at  $\frac{1}{4}$ -span, mid-span and  $\frac{3}{4}$ -span. A full bridge closure was not permitted so the test  
560 was carried out early in the morning when there was little traffic. Ideally, the truck would  
561 stay parked at a given location for as long as possible, because the longer the time series the  
562 more accurate the subsequent modal analysis is likely to be. However, the fact there was no  
563 bridge closure meant that the stops had to be kept relatively short. Only stop durations of 10-  
564 12 s were feasible. However, signals of this length are sufficiently long to allow the modal  
565 properties to be determined accurately.

566



567 Fig. 10: Dimensions and instrumentation details for Bridge B (a) Plan view of bridge deck  
 568 and sensor locations; (b) Accelerometer attached to underside of the girder top flange.

569

## 570 4.2 Evolution of Vehicle-Bridge system

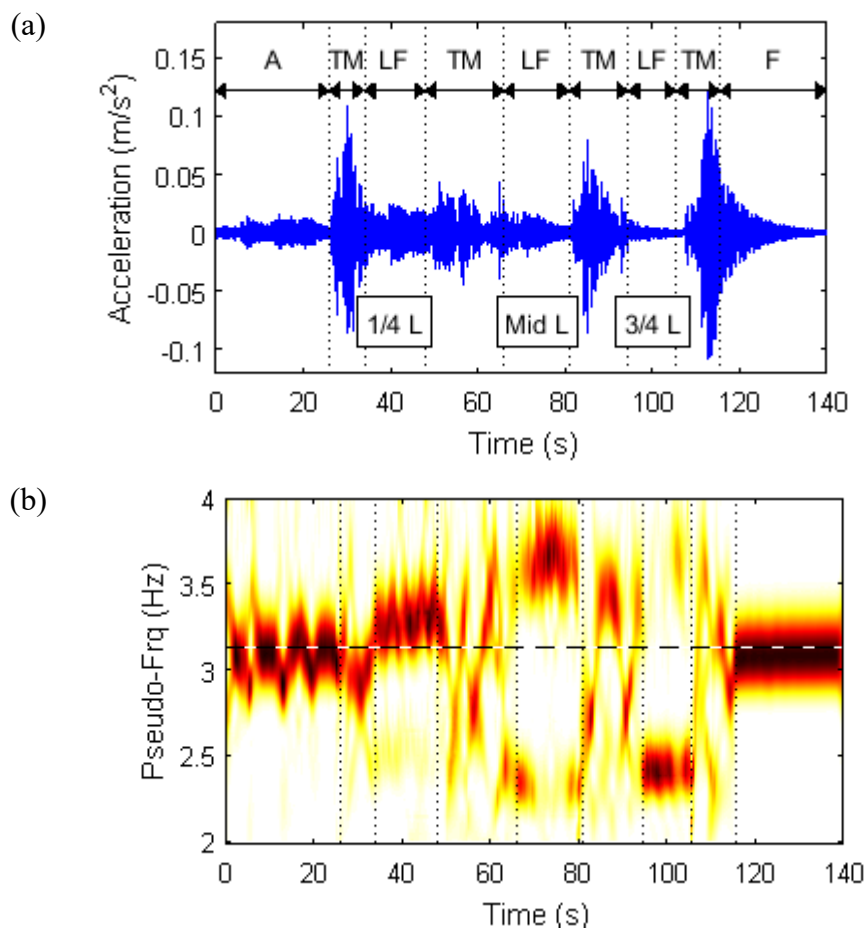
571

572 Analysing the ambient vibration data, the fundamental (first bending) frequency of the bridge  
 573 was identified as 3.13 Hz. Fig. 11(a) shows the time series recorded at accelerometer B for a  
 574 full set of truck movements, namely; truck coming on to the bridge, parking at  $\frac{1}{4}$ -span,  
 575 moving on and parking at mid-span, then finally moving to  $\frac{3}{4}$ -span and parking briefly before  
 576 exiting the bridge. The different portions of the signal are demarcated using vertical dotted  
 577 lines and the parts of the signal corresponding to the truck being parked at particular locations  
 578 on the bridge can be identified using the annotations on the bottom of the figure. The  
 579 annotations on the top of the figure have been added to allow the reader visualise what the  
 580 truck is doing for each section of the signal. For the first 25 seconds the bridge is in ambient  
 581 vibration (A). Then the truck moves (TM) on to the bridge arriving at the  $\frac{1}{4}$ -span at  
 582 approximately 35 s. On arrival at  $\frac{1}{4}$ -span the truck stops and remains there for approximately  
 583 12 seconds and this section of the signal is termed 'loaded free vibration (LF)'. TM and LF  
 584 are repeated in sequence so that the truck can be parked for a short duration at mid-span and  
 585  $\frac{3}{4}$ -span. When the truck leaves the bridge, the bridge is in free vibration (F). For the data  
 586 presented in Fig. 11 the only vehicle on the bridge was the test truck, i.e. there was no other  
 587 traffic crossing the bridge. Much of the bridge vibration evident in the figure is believed to be  
 588 due to the energy input into the bridge during the four truck movements..

589

590 To observe how the bridge frequency evolves over the course of the truck movements, the  
 591 time series in Fig. 11(a) is analysed using CWT, and the results are presented in Fig. 11(b).

592 Again, the vertical dotted lines demarcate the different parts of the signal (i.e. the lines  
 593 correspond to those shown in part (a) of the figure) and it can be seen that during ambient  
 594 vibration at the start of the signal the bridge vibrates predominantly at its unloaded  
 595 fundamental frequency (3.13 Hz) with no significant energy at any other frequency. The  
 596 same is true for the free vibration at the end of the signal. During the four truck movement  
 597 phases (TM) there is no clear pattern of the energy distribution in the time-frequency domain.  
 598 However, during the loaded free vibration events (LF), the energy is concentrated along clear  
 599 frequency bands. For example, when the truck is parked at mid-span (65-81 s) the energy is  
 600 concentrated in two distinct bands at approximately 2.5 Hz and 3.5 Hz. Similarly, when the  
 601 truck is at the  $\frac{3}{4}$ -point (95-105 s) it can be seen that there is significant energy at these bands  
 602 with almost no energy at the fundamental frequency, indicated by the horizontal dashed line  
 603 in the figure.  
 604

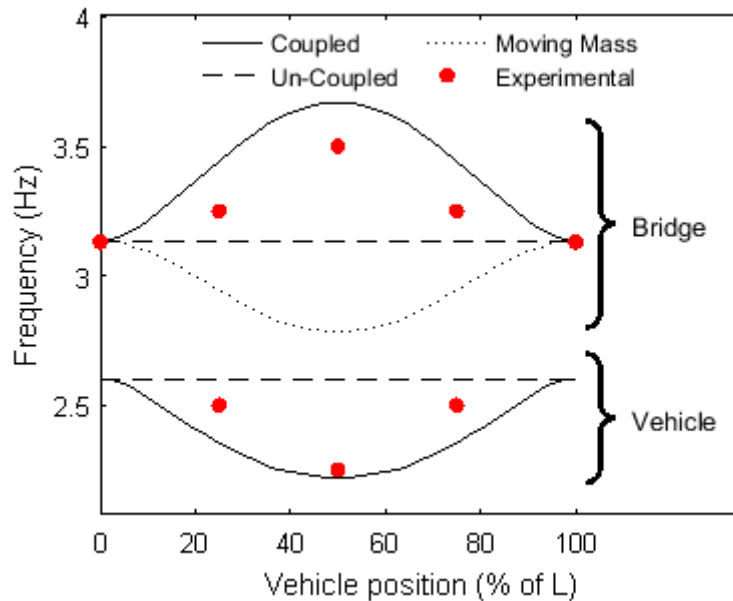


605 Fig. 11: Experimental data from Bridge B; (a) acceleration signal recorded at mid-span  
 606 during a series of truck movements; (b) CWT of acceleration signal; Vertical lines = start/end  
 607 of forcing regime; Horizontal dashed lines = bridge's fundamental frequencies

608  
609  
610  
611  
612  
613  
614  
615  
616  
617  
618  
619  
620  
621  
622  
623  
624  
625  
626  
627  
628  
629  
630  
631

While the CWT plot shown in Fig. 11(b) is useful to visualise the frequency shift for the different truck positions, its frequency resolution is limited. To identify the frequencies more accurately the LF portions of the signal when the truck is at  $\frac{1}{4}$ -span, mid-span and  $\frac{3}{4}$ -span are analysed using FDD and the identified frequencies are plotted as circular data markers at 25%, 50% and 75% of L respectively, in Fig. 12. The experimental results indicate that the bridge and vehicle frequencies increase and decrease respectively when the truck is on the bridge with the largest changes occurring when the truck is in the centre of the bridge. The upper and lower (solid) lines in Fig. 12 respectively show the bridge and vehicle frequencies predicted by the numerical model described in Section 2.1, for a simply supported single span beam. In line with the modelling philosophy described in Section 3.3, the bridge properties in the model were revised so that the uncoupled bridge frequency in the model matches the experimentally observed fundamental bridge frequency (3.13 Hz). A similar approach is also used to revise vehicle properties. Based on the extracted values in Fig. 12 an uncoupled vehicle frequency in the region of 2.6 Hz seems sensible. Therefore the suspension property of the vehicle model (i.e. the spring stiffness) has been amended such that for a sprung mass of 32,000 kg the uncoupled vehicle frequency is 2.6 Hz. As the numerical model is a relatively simple, the frequencies predicted by the model do not exactly match the frequencies observed experimentally. However, the comparison highlights that the trends are the same. This is important because it demonstrates that the evolution of the system frequencies (bridge and vehicle) predicted by the model are credible. Moreover, it shows that the hypothesis put forward in Section 2.3 to explain the behaviour observed in Bridge A is also credible.





632

633 Fig. 12: Frequency evolution during vehicle passage. Solid line = Coupled system; Dashed

634 line = uncoupled system; Dotted line = Moving mass case; Red dots = experimental values

635

636 Finally, the dotted plot in Fig. 12 shows the bridge frequency predicted by the numerical

637 model if an un-sprung mass of 32,000 kg is placed at a series of discrete locations along the

638 length of the bridge. The model predicts that for an un-sprung mass the bridge frequency will

639 be reduced, with the largest reduction occurring when the mass is at the centre of the bridge.

640 This reduction in frequency with the addition of mass is in line with what one might

641 intuitively expect for a (sprung) truck but this is clearly not what actually occurs.

642

### 643 4.3 Modes of vibration

644

645 So far previous sections have focused on studying how different truck positions affect the

646 frequencies of the vehicle-bridge system. In this section, changes in the associated mode

647 shapes of the vehicle-bridge system are reported. To make sense of the theoretical frequency

648 predictions presented in Fig. 7 the reader was prompted to visualise the body mass of the

649 vehicle as supported on two springs, the upper spring representing the vehicle suspension and

650 lower spring representing the bridge stiffness. While this is a useful analogy to visualise what

651 is happening it is technically incorrect because the lower spring is in fact a beam. The

652 significance of this is that when the sprung mass is on the bridge, the frequency that we have

653 been referring to up to now as the vehicle frequency will have a mode associated with it that

654 includes the deformed shape of the beam.

655

656 Up to now this paper has talked about ‘vehicle’ frequency and ‘bridge’ frequency because  
657 based on conventional thinking it is the most straightforward way to explain the experimental  
658 results that have been reported so far. However, to understand the modes associated with the  
659 observed frequencies it is important to appreciate that as soon as the vehicle is on the bridge,  
660 the vehicle and the bridge behave as one system, not two independent systems. Therefore,  
661 technically it is not appropriate to talk about vehicle and bridge modes, it would be more  
662 correct to talk about the coupled system’s first and second mode. However, for simplicity and  
663 convention, when presenting the relevant modes below they will still be referred to as  
664 ‘vehicle mode’ and ‘bridge mode’ even though it is not totally correct.

665

666 The easiest way to appreciate the mode of vibration of the coupled system is to examine the  
667 modes predicted by the numerical model. In particular, Fig. 13 shows the modes of vibration  
668 for three different vehicle locations; (i) over the left support, (ii)  $\frac{1}{4}$ -span and (iii) mid-span.  
669 The eigenvalue analysis of the coupled system is carried out and modal ordinates of the  
670 degrees of freedom of the vehicle and bridge can easily be computed. When the vehicle is at  
671 the bridge’s left support, both systems are effectively uncoupled and the familiar  
672 (independent) modes for the vehicle (Fig. 13(a)) and bridge (Fig. 13(b)) are observed. In  
673 particular note how the bridge part of the ‘vehicle mode’ (Fig. 13(a)) remains straight.  
674 However, when the vehicle is at  $\frac{1}{4}$ -span the bridge clearly plays a role in the ‘vehicle mode’  
675 as the bridge is now in a curved shape (see Fig. 13(c)). Interestingly when the vehicle is at  $\frac{1}{4}$ -  
676 span the deformed shape of the bridge is approximately similar for both the ‘vehicle mode’  
677 (Fig. 13(c)), and the ‘bridge mode’ (Fig. 13(d)). A similar pattern is observed when the  
678 vehicle is at mid-span Figs. 13 (e) and (f).

679

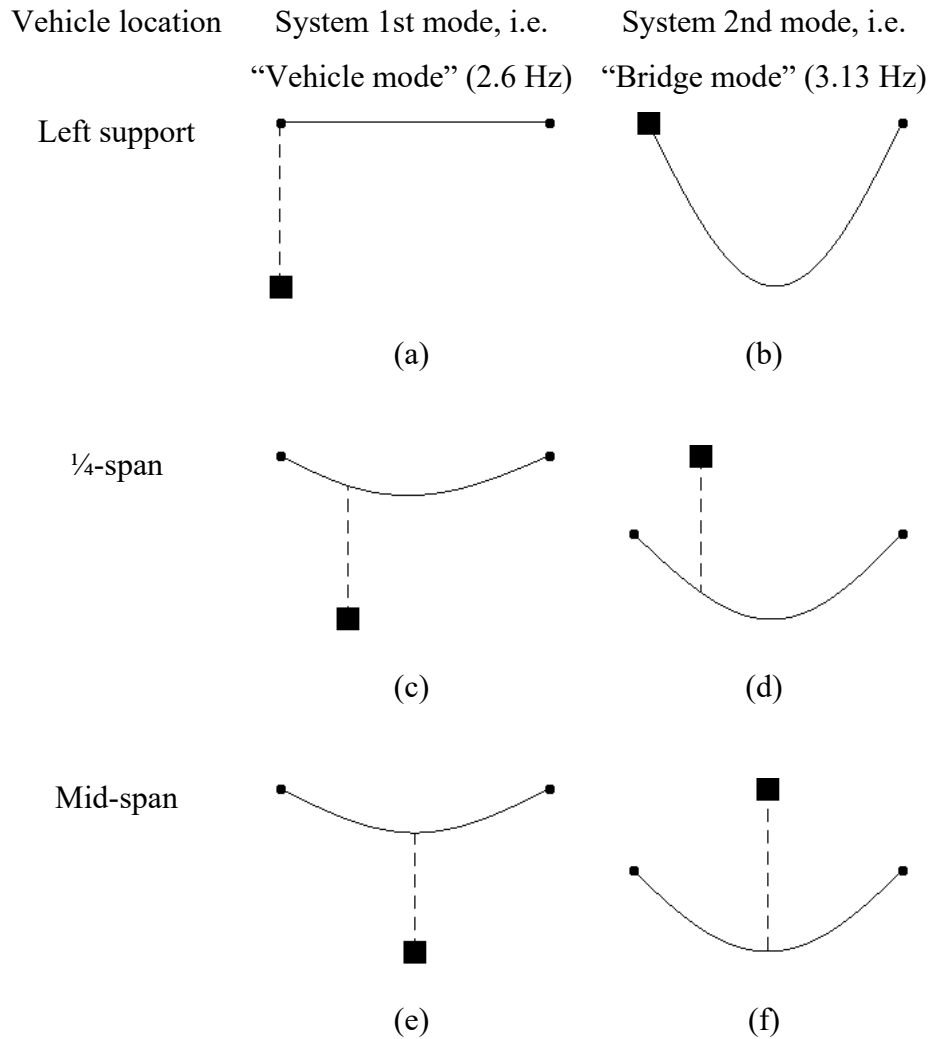


Fig. 13: Numerical mode evolution for coupled system

680

681

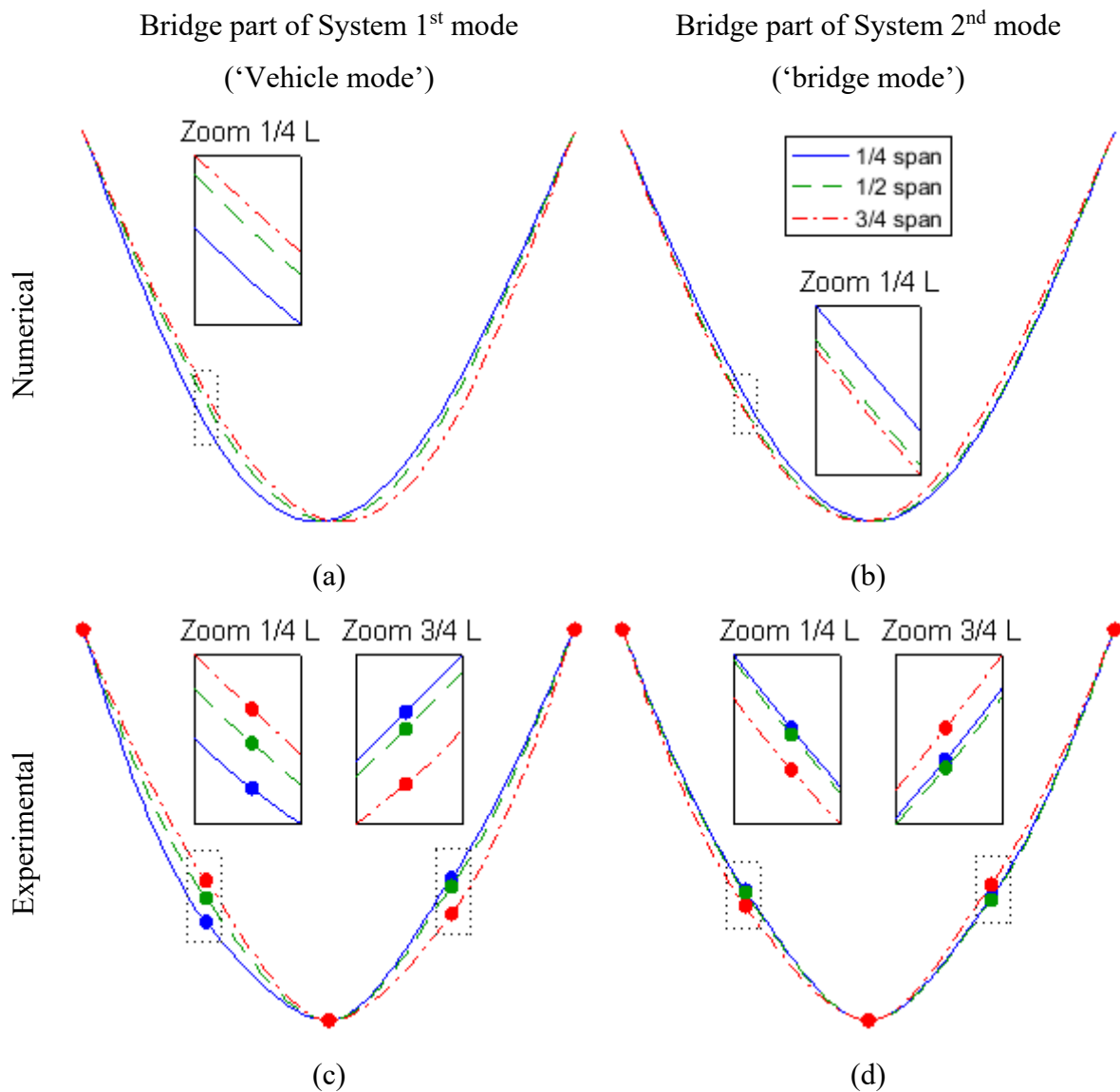
682 It should be noted that the modes of vibration plotted in Fig. 13 are schematic in nature. Their  
683 primary purpose is to demonstrate that when the vehicle is on the bridge the system is  
684 coupled. The resulting modes can be more usefully thought of as the system’s 1<sup>st</sup> and 2<sup>nd</sup>  
685 modes. To examine in more detail how the bridge part of the full system modes of vibration  
686 vary with truck position, just the bridge part of the 1<sup>st</sup> and 2<sup>nd</sup> system modes are plotted in  
687 Fig. 14. Since no acceleration was measured on the vehicle, only the bridge part of the mode  
688 can be examined in detail. Parts (a), (b) and (c), (d) of Fig. 14 are generated using the  
689 numeric model and experimental data respectively. The bridge part of the system 1<sup>st</sup> mode  
690 (‘vehicle mode’) predicted by the numerical model for three different truck positions (1/4-  
691 span, mid-span, and 3/4-span) are plotted in Fig. 14(a). In the figure it can be seen that the  
692 bridge part of the ‘vehicle mode’ has three distinct shapes for the three different truck  
693 locations considered. When the truck is at 1/4-span the bridge part of the mode is slightly

694 skewed to the left, for the  $\frac{3}{4}$ -span position it is skewed to the right and when the vehicle is at  
695 mid-span it is symmetric. Fig. 14(c) shows the equivalent modal ordinates obtained  
696 experimentally and for the three test points. Admittedly as the experiment only provides three  
697 modal ordinates it is not possible to make definitive comment on whether the mode shapes  
698 are skewed or not. However, for the three modal ordinates available, we can observe that they  
699 are behaving in a manner consistent with the equivalent location of the theoretical mode  
700 shapes shown in Fig. 14(a).

701

702 Fig. 14(b) shows the bridge part of the system 2<sup>nd</sup> mode ('bridge mode') predicted by the  
703 numerical model for three different truck positions. It can be seen in the figure that the bridge  
704 part of the system 2<sup>nd</sup> mode does not change significantly with vehicle position but there is  
705 some small variation. Essentially, the numerical model indicates that the bridge part of the  
706 mode is slightly skewed to the opposite side of where the vehicle is located. The equivalent  
707 experimental modal ordinates are plotted in Fig. 14(d). Similar to Fig. 14(c), in Fig. 14(d)  
708 only three modal ordinates are available and therefore there is insufficient evidence to  
709 determine if the subtle skewing of modes evident in Fig. 14(b) is also present experimentally.  
710 However, it can be said that the magnitude of the modal ordinates at a given location are  
711 quite similar for all three truck positions. This is consistent with the theoretical modes  
712 presented in Fig. 14(b) which as mentioned previously appear relatively insensitive to vehicle  
713 position. Note that all the plots in Fig. 14 have been normalized to have a minimum value of -  
714 1 at mid-span for ease of comparison.

715



716 Fig. 14: Bridge part of system 1<sup>st</sup> and 2<sup>nd</sup> modes for different truck positions (a) 1<sup>st</sup> mode  
 717 calculated theoretically, (b) 2<sup>nd</sup> mode calculated theoretically, (c) 1<sup>st</sup> mode  
 718 experimentally, (d) 2<sup>nd</sup> mode measured experimentally.

719

## 720 5. Conclusions

721

722 This paper investigated the changes in frequencies and modes of vibration of a vehicle-bridge  
 723 system. Two different bridges A and B were studied. Initial experimental results observed on  
 724 bridge A included some unexpected behaviour. In particular when the truck was on the bridge  
 725 the fundamental bridge frequency seemed to increase and a frequency peak not present in free  
 726 vibration appeared on the spectrum. This prompted the development of a numerical model to  
 727 try and provide a theoretical explanation for the observed behaviour. The model provided a  
 728 theoretical framework which seemed to explain the observed behaviour. However, to further

729 investigate the phenomena a second experiment was carried out where the truck parked at a  
730 series of discrete locations on the bridge. This experiment was carried out on Bridge B and,  
731 by using time-frequency analysis and output-only modal analysis, the unexpected behaviour  
732 was further clarified.

733

734 Furthermore, in the course of the investigation a number of interesting observations were  
735 made. For example, a coupled vehicle-bridge system might feature significant changes in  
736 natural frequencies depending on the vehicle's position. Also when analysing forced  
737 vibration signals the presence of additional frequencies on the spectrum proves system  
738 coupling. Moreover, it is shown numerically and experimentally, that the modes of vibration  
739 of the coupled system do change with the location of the vehicle. However, the amount of  
740 change differs for the 'vehicle' and the 'bridge' modes. In particular, it is shown that when  
741 the vehicle is on the bridge the 'vehicle' mode has a significant 'bridge part' associated with  
742 it and the shape of this part is very similar to the bridge's fundamental mode of vibration.

743

744 Numeric models indicate the magnitude of the changes in modal parameters will be more  
745 pronounced for situations with high vehicle-bridge mass ratios. However, this paper shows  
746 that it is a reality for conventional heavy vehicles and relatively light standard bridges.

747

#### 748 **Acknowledgements**

749

750 The research leading to these results has received funding from the People Programme  
751 (Marie Curie Actions) of the European Union's Seventh Framework Programme (FP7/2007-  
752 2013) under grant agreement n° 330195. The authors would also like to thank John Vittery of  
753 EM Highways Services Limited, and the Bridge Section of The Engineering Design Group of  
754 Devon County Council led by Kevin Dentith BSc, CEng, FICE, for their support and  
755 assistance with this work.

756

#### 757 **References**

758

759 [1] E.B. Magrab, Vibrations of Elastic Systems – With Applications to MEMS and NEMS,  
760 Springer, Dordrecht, 2012.

761

- 762 [2] L. Frýba, *Vibration of Solids and Structures under Moving Loads*, third ed., Thomas  
763 Telford, Prague, 1999.  
764
- 765 [3] Y.B. Yang, M.C. Cheng, K.C. Chang, Frequency variation in vehicle-bridge interaction  
766 systems, *Int. J. Struct. Stab. Dyn.* 13 (2013) 1-22.  
767
- 768 [4] J. Li; M. Su; and L. Fan, Natural frequency of railway girder bridges under vehicle loads,  
769 *J. Bridge Eng.* 8 (2003) 199-203.  
770
- 771 [5] D. Cantero, E.J. OBrien, The non-stationarity of apparent bridge natural frequencies  
772 during vehicle crossing events, *FME Trans.* 41 (2013) 279-284.  
773
- 774 [6] K.C. Chang, C.W. Kim, S. Borjigin, Variability in bridge frequency induced by a parked  
775 vehicle, *Smart Struct. Syst.* 13 (2014) 755-773.  
776
- 777 [7] M.D. Spiridonakos, S.D. Fassois, Parametric identification of time-varying structure  
778 based on vector vibration response measurements, *Mech. Syst. Sig. Process.* 23 (2009) 2029-  
779 2048.  
780
- 781 [8] C.Y. Kim, D.S. Jung, N.S. Kim, S.D. Kwon, M.Q. Feng, Effect of vehicle weight on  
782 natural frequencies of bridges measured from traffic-induced vibration. *Earthquake Eng. Eng.*  
783 *Vibr.* 2 (2003) 109-115.  
784
- 785 [9] F. Xiao, G.S. Chen, J.Leroy Hulsey, W. Zatar, Characterization of non-stationary  
786 properties of vehicle-bridge response for structural health monitoring, *Adv. Mech. Eng.* 9  
787 (2017) 1-6.  
788
- 789 [10] C.C. Caprani, E. Ahmadi, Formulation of human–structure interaction system models for  
790 vertical vibration, *J. Sound Vib.* 377 (2016) 346-367.  
791
- 792 [11] X. Kong, C.S. Cai, B. Kong, Numerically extracting bridge modal properties from  
793 dynamic responses of moving vehicles, *ASCE J. Eng. Mech.* 142 (2016) 1-12  
794

795 [12] E.J. OBrien, A. Malekjafarian. A mode shape-based damage detection approach using  
796 laser measurement from a vehicle crossing a simply supported bridge, *Struct. Control Health*  
797 *Monit.* 23 (2016) 1273-1286.  
798

799 [13] D.M. Siringoringo, Y. Fujino, Estimating bridge fundamental frequency from vibration  
800 response of instrumented passing vehicle: analytical and experimental study, *Adv. Struct.*  
801 *Eng.* 15 (2012) 417-433.  
802

803 [14] Matlab, MathWorks, 2013.  
804

805 [15] O.C. Zienkiewicz, R.L. Taylor, *The Finite Element Method – Volume 1: The Basis*, fifth  
806 ed., Butterworth Heinemann, Oxford, 2000.  
807

808 [16] P. Lou. Finite element analysis of train-track-bridge interaction system, *Arch. Appl.*  
809 *Mech.* 77 (2007) 707-728.  
810

811 [17] Y.B. Yang, J.D. Yau, Y.S. Wu, *Vehicle-Bridge Interaction Dynamics – With*  
812 *Applications to High-Speed Railways*, World Scientific, Singapore, 2004.  
813

814 [18] L. Gyenes, C.G.B. Mitchell, S.D. Phillips, Dynamic pavement loads and tests of road-  
815 friendliness for heavy vehicle suspensions, in: D. Cebon, C.G.B. Mitchell (Eds.), *Heavy*  
816 *Vehicles and Roads: Technology, Safety and Policy*, Thomas Telford, London, 1992, pp.  
817 243-251.  
818

819 [19] D.J. Ewins, *Modal Testing. Theory, Practice and Application.* second ed., Research  
820 *Studies Press LTD*, Baldock, 2000.  
821

822 [20] C. Rainieri, G. Fabbrocino, *Operational Modal Analysis of Civil Engineering Structures.*  
823 *An Introduction and Guide for Applications*, Springer, New York, 2014.  
824

825 [21] A. Cohen, R.D. Ryan, *Wavelets and Multiscale Signal Processing*, Chapman & Hall,  
826 London, 1995.  
827



- 828 [22] S.G. Mallat, A Wavelet Tour of Signal Processing, second ed., Academic Press, London,  
829 1999.  
830
- 831 [23] D. Cantero, M. Ülker-Kaustell, R. Karoumi. Time–frequency analysis of railway bridge  
832 response in forced vibration, *Mech. Syst. Sig. Process.* 76-77 (2016) 518–530.  
833
- 834 [24] Y.B. Yang, C.W. Lin, J.D. Yau, Extracting bridge frequencies from the dynamic  
835 response of passing vehicle. *J. Sound Vib.* 2072 (2004) 471-493.  
836
- 837 [25] R. Cantieni, Investigation of vehicle-bridge interaction for highway bridges. In: *Heavy*  
838 *Vehicles and Roads: Technology, Safety and Policy*, Thomas Telford, London, 1992.  
839
- 840 [26] H. Ludescher, E. Brühwiler, Dynamic amplification of traffic loads on road bridges,  
841 *Struct. Eng. Int.* 19 (2009) 190-197.  
842